

# QUATERNION TENSOR RING DECOMPOSITION AND APPLICATION FOR COLOR IMAGE INPAINTING \*

JIFEI MIAO<sup>†</sup> AND KIT IAN KOU<sup>‡</sup>

**Abstract.** In recent years, tensor networks have emerged as powerful tools for solving large-scale optimization problems. One of the most promising tensor networks is the tensor ring (TR) decomposition, which achieves circular dimensional permutation invariance in the model through the utilization of the trace operation and equitable treatment of the latent cores. On the other hand, more recently, quaternions have gained significant attention and have been widely utilized in color image processing tasks due to their effectiveness in encoding color pixels. Therefore, in this paper, we propose the quaternion tensor ring (QTR) decomposition, which inherits the powerful and generalized representation abilities of the TR decomposition while leveraging the advantages of quaternions for color pixel representation. In addition to providing the definition of QTR decomposition and an algorithm for learning the QTR format, this paper also proposes a low-rank quaternion tensor completion (LRQTC) model and its algorithm for color image inpainting based on the QTR decomposition. Finally, extensive experiments on color image inpainting demonstrate that the proposed QTLRC method is highly competitive.

**Key words.** Quaternion tensor ring decomposition, quaternion tensor low-rank completion, color image inpainting

**MSC codes.**

**1. Introduction.** Tensor networks have gained prominence in recent years as powerful tools for tackling large-scale optimization problems [10, 4, 17, 30, 31]. Among them, the tensor ring (TR) decomposition [30] is one of the most advanced tensor networks. The TR decomposition is a method that represents an  $N$ -th order tensor  $\mathcal{T} \in \mathbb{R}^{I_1 \times I_2 \times \dots \times I_N}$  by multiplying a sequence of third-order tensors  $\mathcal{Z}_n$ ,  $n = 1, 2, \dots, N$  in a circular manner. Specifically, it can be expressed in an element-wise form given by

$$\mathcal{T}(i_1, i_2, \dots, i_N) = \text{Tr}\{\mathcal{Z}_1(i_1)\mathcal{Z}_2(i_2)\dots\mathcal{Z}_N(i_N)\},$$

where  $\mathcal{T}(i_1, i_2, \dots, i_N)$  denotes the  $(i_1, i_2, \dots, i_N)$ -th element of  $\mathcal{T}$ ,  $\text{Tr}\{\cdot\}$  denotes the trace operator,  $\mathcal{Z}_n(i_n) \in \mathbb{R}^{r_n \times r_{n+1}}$  denotes the  $i_n$ -th lateral slice of  $\mathcal{Z}_n$ , the last  $\mathcal{Z}_N$  is of size  $r_N \times I_N \times r_1$ , *i.e.*,  $r_{N+1} = r_1$ . The TR decomposition has been widely utilized in various image processing tasks due to its powerful and generalized representation ability. In particular, the TR-based low-rank tensor completion (LRTC) methods for image inpainting have been extensively studied recently [26, 7, 19, 23].

On the other hand, quaternions have gained considerable attention in the field of color image processing as a more suitable tool for representing color pixels. Concretely, the quaternion-based method encodes the RGB three-channel pixel values on the three imaginary parts of a quaternion [11]. That is

$$(1.1) \quad \vec{t} = 0 + t_r i + t_g j + t_b k,$$

---

\*Submitted to the editors DATE.

**Funding:** This work was funded by University of Macau (File no. MYRG2019-00039-FST, MYRG2022-00108-FST), Science and Technology Development Fund, Macau S.A.R (File no.FDCT/0036/2021/AGJ).

<sup>†</sup>The School of Mathematics and Statistics, Yunnan University, Kunming, Yunnan, 650091, China (jifmiao@163.com).

<sup>‡</sup>The Department of Mathematics, Faculty of Science and Technology, University of Macau, Macau 999078, China (kikou@umac.mo).

where  $\hat{t}$  denotes a color pixel,  $t_r$ ,  $t_g$ , and  $t_b$  are RGB three-channel pixel values,  $i$ ,  $j$ , and  $k$  are the three imaginary units. While both real-valued third-order tensors and quaternion matrices can be utilized for representing color images, quaternion matrices, being a novel representation, possess more favorable characteristics and advantages in this context. When dealing with color pixels comprising RGB channels, real-valued third-order tensors may not fully exploit the strong correlation among the three channels. This limitation arises from the fact that real-valued third-order tensors represent color images by simply concatenating the RGB channels together, treating both the “intra-channel relationship” (the relationship within each channel) and the “spatial relationship” (the relationship between pixels) equally [16]. In contrast, quaternions treat the three channels of color pixels as a cohesive entity [13, 14, 9, 3], thereby effectively preserving the intra-channel relationship. Hence, quaternion matrices and quaternion tensors, particularly their low-rank approximation models, have been extensively utilized for color image processing tasks recently. For instance, quaternion matrix rank minimization methods [9, 3, 8, 24], quaternion matrix factorization methods [12, 13], and quaternion tensor-based methods [14, 18, 16]. These methods have achieved remarkable results in tasks such as color image inpainting and color image denoising.

While there has been a significant amount of research progress on quaternion matrices recently, the study on quaternion tensors has just begun, particularly in the context of quaternion tensor networks, which remains largely unexplored. Therefore, in this paper, we propose the quaternion tensor ring (QTR) decomposition, which inherits the powerful and generalized representation abilities of the TR decomposition while leveraging the advantages of quaternions for color pixel representation. Therefore, in this paper, we aim to propose the quaternion tensor ring (QTR) decomposition, which will inherit the powerful and generalized representation capabilities of the TR decomposition while leveraging the advantages of quaternions for color pixel representation. However, due to the non-commutativity of quaternion multiplication, the definition and associated properties of QTR differ from TR. This distinction is the reason why QTR is introduced as a separate concept from TR.

We summarize the main contributions of this paper as follows:

- We define the QTR decomposition for quaternion tensors and prove its cyclic permutation property. Furthermore, inspired by the TR-SVD algorithm introduced in [30], we also present the QTR-QSVD algorithm for learning the QTR format.
- We define the quaternion tensor circular unfolding and prove the relationship between the rank of these unfolding matrices and the QTR-rank. Based on this, we propose a low-rank quaternion tensor completion (LRQTC) model along with its corresponding computational method.
- We extend a tensor augmentation technique called OKA [28] to quaternion matrices, enabling the transformation of quaternion matrices into higher-order quaternion tensors. Subsequently, we apply the proposed LRQTC method to color image inpainting tasks. Experimental results validate the competitiveness of the proposed approach.

The remainder of this paper is organized as follows. Section 2 introduces some notations and preliminaries for quaternion algebra, including quaternion matrices and quaternion tensors.

## 2. Preliminary.

**2.1. Notations.** In this paper,  $\mathbb{R}$ ,  $\mathbb{C}$ , and  $\mathbb{H}$  respectively denote the real space, complex space, and quaternion space. A scalar, a vector, a matrix, and a tensor are written as  $a$ ,  $\mathbf{a}$ ,  $\mathbf{A}$ , and  $\mathcal{A}$  respectively.  $\dot{a}$ ,  $\dot{\mathbf{a}}$ ,  $\dot{\mathbf{A}}$ , and  $\dot{\mathcal{A}}$  respectively represent a quaternion scalar, a quaternion vector, a quaternion matrix, and a quaternion tensor.

**2.2. Introduction to quaternions.** Quaternion was introduced by Hamilton [5]. A quaternion  $\dot{q} \in \mathbb{H}$  has a Cartesian form given by:

$$(2.1) \quad \dot{q} = q_0 + q_1 i + q_2 j + q_3 k,$$

where  $q_l \in \mathbb{R}$  ( $l = 0, 1, 2, 3$ ) are called its components,  $i$ ,  $j$ , and  $k$  are the three imaginary units related through the famous relations:

$$(2.2) \quad \begin{cases} i^2 = j^2 = k^2 = ijk = -1, \\ ij = -ji = k, jk = -kj = i, ki = -ik = j. \end{cases}$$

Quaternions have similar rules for addition, subtraction, multiplication, and division as complex numbers, as well as similar definitions for conjugation and modulus. However, the difference lies in the non-commutativity property of quaternion multiplication. That is, in general  $\dot{p}\dot{q} \neq \dot{q}\dot{p}$ .

A multidimensional array or an  $N$ -th order tensor is named a quaternion tensor if its elements are quaternion numbers (quaternion matrices can be regarded as second-order quaternion tensors), *i.e.*,  $\dot{\mathcal{T}} = (\dot{t}_{i_1 i_2 \dots i_N}) \in \mathbb{H}^{I_1 \times I_2 \times \dots \times I_N} = \mathcal{T}_0 + \mathcal{T}_1 i + \mathcal{T}_2 j + \mathcal{T}_3 k$ , where  $\mathcal{T}_l \in \mathbb{R}^{I_1 \times I_2 \times \dots \times I_N}$  ( $l = 0, 1, 2, 3$ ),  $\dot{\mathcal{T}}$  is pure if  $\mathcal{T}_0$  is a zero tensor [14]. Then, we extend three unfolding methods for real tensors in [30] to quaternion tensors.

**DEFINITION 2.1.** *Multi-index operation [19]: The multi-index operation is defined as follows:*

$$\overline{i_1 i_2 \dots i_N} = i_1 + (i_2 - 1)I_1 + (i_3 - 1)I_1 I_2 + \dots + (i_N - 1) \prod_{n=1}^{N-1} I_n,$$

where  $i_n \in [I_n]$ .

**DEFINITION 2.2.  $k$ -unfolding:** Let  $\dot{\mathcal{T}} \in \mathbb{H}^{I_1 \times I_2 \times \dots \times I_N}$  be an  $N$ -th order quaternion tensor, the  $k$ -unfolding of  $\dot{\mathcal{T}}$  is a quaternion matrix, denoted by  $\dot{\mathbf{T}}_{(k)}$  of size  $\prod_{n=1}^k I_n \times \prod_{n=k+1}^N I_n$ , whose elements are defined by

$$\dot{\mathbf{T}}_{(k)}(m, n) = \dot{\mathcal{T}}(i_1, i_2, \dots, i_N),$$

where  $m = \overline{i_1 i_2 \dots i_k}$ ,  $n = \overline{i_{k+1} i_{k+2} \dots i_N}$ .

**DEFINITION 2.3. mode- $k$  unfolding:** Let  $\dot{\mathcal{T}} \in \mathbb{H}^{I_1 \times I_2 \times \dots \times I_N}$  be an  $N$ -th order quaternion tensor, the mode- $k$  unfolding of  $\dot{\mathcal{T}}$  is a quaternion matrix, denoted by  $\dot{\mathbf{T}}_{[k]}$  of size  $I_k \times \prod_{n \neq k} I_n$ , whose elements are defined by

$$\dot{\mathbf{T}}_{[k]}(i_k, t) = \dot{\mathcal{T}}(i_1, i_2, \dots, i_N),$$

where  $t = \overline{i_{k+1} \dots i_N i_1 \dots i_{k-1}}$ .

**DEFINITION 2.4. classical mode- $k$  unfolding:** Let  $\dot{\mathcal{T}} \in \mathbb{H}^{I_1 \times I_2 \times \dots \times I_N}$  be an  $N$ -th order quaternion tensor, the classical mode- $k$  unfolding of  $\dot{\mathcal{T}}$  is a quaternion matrix, denoted by  $\dot{\mathbf{T}}_{(k)}$  of size  $I_k \times \prod_{n \neq k} I_n$ , whose elements are defined by

$$\dot{\mathbf{T}}_{(k)}(i_k, t) = \dot{\mathcal{T}}(i_1, i_2, \dots, i_N),$$

where  $t = \overline{i_1 \dots i_{k-1} i_{k+1} \dots i_N}$ .

In order to provide the definition of QTR decomposition, we will first introduce two types of quaternion matrix product.

**DEFINITION 2.5.** *Left and right quaternion matrix products [20]: Given two quaternion matrices  $\dot{\mathbf{A}} \in \mathbb{H}^{M \times N}$  and  $\dot{\mathbf{B}} \in \mathbb{H}^{N \times P}$ , the left and right products are respectively defined as*

$$(2.3) \quad (\dot{\mathbf{A}} \cdot_L \dot{\mathbf{B}})_{mp} = \sum_{n=1}^N \dot{a}_{mn} \dot{b}_{np} \quad \text{and} \quad (\dot{\mathbf{A}} \cdot_R \dot{\mathbf{B}})_{mp} = \sum_{n=1}^N \dot{b}_{np} \dot{a}_{mn}.$$

Note that due to the non-commutativity of quaternion multiplication, generally  $\dot{\mathbf{A}} \cdot_L \dot{\mathbf{B}} \neq \dot{\mathbf{A}} \cdot_R \dot{\mathbf{B}}$ . For simplicity, we also define  $\dot{a} \cdot_L \dot{b} = \dot{a}\dot{b}$  and  $\dot{a} \cdot_R \dot{b} = \dot{b}\dot{a}$  for quaternion scalars  $\dot{a}$  and  $\dot{b}$ . Additionally, if we do not specify whether it is left product or right product, it is assumed to be left product, *i.e.*,  $\dot{\mathbf{A}}\dot{\mathbf{B}} = \dot{\mathbf{A}} \cdot_L \dot{\mathbf{B}}$ . The defined left and right quaternion matrix products have the following associativity property [21]:

$$(\dot{\mathbf{A}} \cdot_L \dot{\mathbf{B}}) \cdot_L \dot{\mathbf{C}} = \dot{\mathbf{A}} \cdot_L (\dot{\mathbf{B}} \cdot_L \dot{\mathbf{C}}) \quad \text{and} \quad (\dot{\mathbf{A}} \cdot_R \dot{\mathbf{B}}) \cdot_R \dot{\mathbf{C}} = \dot{\mathbf{A}} \cdot_R (\dot{\mathbf{B}} \cdot_R \dot{\mathbf{C}}).$$

However, in general

$$(\dot{\mathbf{A}} \cdot_L \dot{\mathbf{B}}) \cdot_R \dot{\mathbf{C}} \neq \dot{\mathbf{A}} \cdot_L (\dot{\mathbf{B}} \cdot_R \dot{\mathbf{C}}) \quad \text{and} \quad (\dot{\mathbf{A}} \cdot_R \dot{\mathbf{B}}) \cdot_L \dot{\mathbf{C}} \neq \dot{\mathbf{A}} \cdot_R (\dot{\mathbf{B}} \cdot_L \dot{\mathbf{C}}).$$

In addition, the property that  $\text{rank}(\dot{\mathbf{A}} \cdot_L \dot{\mathbf{B}}) \leq \min(\text{rank}(\dot{\mathbf{A}}), \text{rank}(\dot{\mathbf{B}}))$  has been proven in [2]. In the following theorem, we demonstrate the same property for the right product of two quaternion matrices.

**THEOREM 2.6.** *For any two quaternion matrices  $\dot{\mathbf{A}} \in \mathbb{H}^{M \times N}$  and  $\dot{\mathbf{B}} \in \mathbb{H}^{N \times P}$ , we have*

$$(2.4) \quad \text{rank}(\dot{\mathbf{A}} \cdot_R \dot{\mathbf{B}}) \leq \min(\text{rank}(\dot{\mathbf{A}}), \text{rank}(\dot{\mathbf{B}})).$$

*Proof.* Denote the right row null spaces of  $\dot{\mathbf{B}}$  and  $\dot{\mathbf{A}} \cdot_R \dot{\mathbf{B}}$  as  $\mathcal{RRN}(\dot{\mathbf{B}}) = \{\dot{\mathbf{x}} \in \mathbb{H}^P : \dot{\mathbf{B}} \cdot_R \dot{\mathbf{x}} = \mathbf{0}\}$  and  $\mathcal{RRN}(\dot{\mathbf{A}} \cdot_R \dot{\mathbf{B}}) = \{\dot{\mathbf{x}} \in \mathbb{H}^P : (\dot{\mathbf{A}} \cdot_R \dot{\mathbf{B}}) \cdot_R \dot{\mathbf{x}} = \mathbf{0}\}$  [21]. One can easily find that  $\mathcal{RRN}(\dot{\mathbf{B}}) \subseteq \mathcal{RRN}(\dot{\mathbf{A}} \cdot_R \dot{\mathbf{B}})$ . Thus,  $\dim \mathcal{RRN}(\dot{\mathbf{B}}) \leq \dim \mathcal{RRN}(\dot{\mathbf{A}} \cdot_R \dot{\mathbf{B}})$  and  $\text{rank}(\dot{\mathbf{A}} \cdot_R \dot{\mathbf{B}}) \leq \text{rank}(\dot{\mathbf{B}})$ . Similarly, Denote the right column null spaces of  $\dot{\mathbf{A}}$  and  $\dot{\mathbf{A}} \cdot_R \dot{\mathbf{B}}$  as  $\mathcal{RCN}(\dot{\mathbf{A}}) = \{\dot{\mathbf{x}} \in \mathbb{H}^M : \dot{\mathbf{x}}^T \cdot_R \dot{\mathbf{A}} = \mathbf{0}^T\}$  and  $\mathcal{RCN}(\dot{\mathbf{A}} \cdot_R \dot{\mathbf{B}}) = \{\dot{\mathbf{x}} \in \mathbb{H}^M : \dot{\mathbf{x}}^T \cdot_R (\dot{\mathbf{A}} \cdot_R \dot{\mathbf{B}}) = \mathbf{0}^T\}$  [21]. One can also find that  $\mathcal{RCN}(\dot{\mathbf{A}}) \subseteq \mathcal{RCN}(\dot{\mathbf{A}} \cdot_R \dot{\mathbf{B}})$ . Thus,  $\dim \mathcal{RCN}(\dot{\mathbf{A}}) \leq \dim \mathcal{RCN}(\dot{\mathbf{A}} \cdot_R \dot{\mathbf{B}})$  and  $\text{rank}(\dot{\mathbf{A}} \cdot_R \dot{\mathbf{B}}) \leq \text{rank}(\dot{\mathbf{A}})$ . In all,  $\text{rank}(\dot{\mathbf{A}} \cdot_R \dot{\mathbf{B}}) \leq \min(\text{rank}(\dot{\mathbf{A}}), \text{rank}(\dot{\mathbf{B}}))$ .  $\square$

**3. Quaternion tensor ring decomposition.** In this section, we will first define the QTR decomposition. Following that, we will present an important property of the QTR decomposition, and finally propose an algorithm for learning the QTR model.

**DEFINITION 3.1.** *QTR decomposition: Let  $\dot{\mathcal{T}} \in \mathbb{H}^{I_1 \times I_2 \times \dots \times I_N}$  be an  $N$ -th order quaternion tensor with  $I_n$ -dimension along the  $n$ -th mode, then QTR representation is to decompose it into a sequence of third-order quaternion tensors  $\dot{\mathcal{Z}}_n \in \mathbb{H}^{r_n \times I_n \times r_{n+1}}$  (which can be also called the  $n$ -th core of  $\dot{\mathcal{T}}$ ),  $n = 1, 2, \dots, N$ , which can be represented using an element-wise formulation as<sup>1</sup>*

$$(3.1) \quad \dot{\mathcal{T}}(i_1, i_2, \dots, i_N) = \text{Tr}\{\dot{\mathcal{Z}}_1(i_1) \cdot_L \dot{\mathcal{Z}}_2(i_2) \cdot_L \dots \cdot_L \dot{\mathcal{Z}}_N(i_N)\},$$

<sup>1</sup>Here we are using left quaternion matrix product, but one can also use right quaternion matrix product for a similar definition.

where  $\dot{\mathcal{T}}(i_1, i_2, \dots, i_N)$  denotes the  $(i_1, i_2, \dots, i_N)$ -th element of  $\dot{\mathcal{T}}$ ,  $\dot{\mathcal{Z}}_n(i_n) = \dot{\mathcal{Z}}_n(:, i_n, :)$   $\in \mathbb{H}^{r_n \times r_{n+1}}$  denotes the  $i_n$ -th lateral slice quaternion matrix of the third-order quaternion tensor  $\dot{\mathcal{Z}}_n$ , the last third-order quaternion  $\dot{\mathcal{Z}}_N$  is of size  $r_N \times I_N \times r_1$ , i.e.,  $r_{N+1} = r_1$ , which ensures the product of these quaternion matrices is a square quaternion matrix. In addition, the vector  $\mathbf{r} = [r_1, r_2, \dots, r_N]$  is defined as the QTR-rank of the quaternion tensor  $\dot{\mathcal{T}}$ .

Note that formula (3.1) can also be expressed in index form as follows:

$$(3.2) \quad \dot{\mathcal{T}}(i_1, i_2, \dots, i_N) = \sum_{\alpha_1=1}^{r_1} \dots \sum_{\alpha_N=1}^{r_N} \dot{\mathcal{Z}}_1(\alpha_1, i_1, \alpha_2) \cdot_L \\ Z_2(\alpha_2, i_2, \alpha_3) \cdot_L \dots \cdot_L Z_N(\alpha_N, i_N, \alpha_{N+1}),$$

where  $\alpha_{N+1} = \alpha_1$ . Thus, one can easily find that quaternion tensor train (QTT) decomposition [15] is a special case of the defined QTR decomposition when  $r_1 = 1$ .

For an efficient representation of QTR decomposition, we first introduce two quaternion tensor products for third-order quaternion tensors, namely the quaternion tensor left connection product and the quaternion tensor right connection product.

**DEFINITION 3.2.** Let  $\dot{\mathcal{Z}}_n \in \mathbb{H}^{r_n \times I_n \times r_{n+1}}$ ,  $n = 1, 2, \dots, N$ , be  $N$  third-order quaternion tensors, the quaternion tensor left connection product and the quaternion tensor right connection product between  $\dot{\mathcal{Z}}_n$  and  $\dot{\mathcal{Z}}_{n+1}$  are respectively defined as

$$(3.3) \quad \dot{\mathcal{Z}}_n \cdot_L \dot{\mathcal{Z}}_{n+1} \in \mathbb{H}^{r_n \times I_n I_{n+1} \times r_{n+2}} = \text{reshape}(\dot{\mathbf{Z}}_n^L \cdot_L \dot{\mathbf{Z}}_{n+1}^R, [r_n, I_n I_{n+1}, r_{n+2}])$$

and

$$(3.4) \quad \dot{\mathcal{Z}}_n \cdot_R \dot{\mathcal{Z}}_{n+1} \in \mathbb{H}^{r_n \times I_n I_{n+1} \times r_{n+2}} = \text{reshape}(\dot{\mathbf{Z}}_n^L \cdot_R \dot{\mathbf{Z}}_{n+1}^R, [r_n, I_n I_{n+1}, r_{n+2}]),$$

where  $\dot{\mathbf{Z}}_n^L \in \mathbb{H}^{r_n I_n \times I_{n+1}} = (\dot{\mathbf{Z}}_n)_{(2)}$  and  $\dot{\mathbf{Z}}_{n+1}^R \in \mathbb{H}^{r_{n+1} \times I_{n+1} I_{n+2}} = (\dot{\mathbf{Z}}_{n+1})_{(1)}$ .

Then, following the definition (3.3), the QTR decomposition (3.1) can be represented as  $\dot{\mathcal{T}} = f(\dot{\mathcal{Z}}) = f(\dot{\mathcal{Z}}_1 \cdot_L \dot{\mathcal{Z}}_2 \cdot_L \dots \cdot_L \dot{\mathcal{Z}}_N)$ , where function  $f$  is a trace operation on  $\dot{\mathcal{Z}}(:, k, :)$ ,  $k = 1, 2, \dots, \prod_{i=1}^N I_i$ , and followed by a reshaping operation from vector of the length  $\prod_{i=1}^N I_i$  to quaternion tensor of the size  $I_1 \times I_2 \times \dots \times I_N$ .

**DEFINITION 3.3.** Quaternion tensor permutation: For any  $N$ -th order quaternion tensor  $\dot{\mathcal{T}} \in \mathbb{H}^{I_1 \times I_2 \times \dots \times I_N}$ , the  $n$ -th quaternion tensor permutation is defined as  $\dot{\mathcal{T}}^{P_n} \in \mathbb{H}^{I_n \times \dots \times I_N \times I_1 \times \dots \times I_{n-1}}$ :

$$(3.5) \quad \dot{\mathcal{T}}^{P_n}(i_n, \dots, i_N, i_1, \dots, i_{n-1}) = \dot{\mathcal{T}}(i_1, i_2, \dots, i_N).$$

In the following theorem, we will present the cyclic permutation property of QTR decomposition.

**THEOREM 3.4.** Cyclic permutation property of QTR decomposition: Based on the definition of quaternion tensor permutation and QTR decomposition, the quaternion tensor permutation of  $\dot{\mathcal{T}}$  is equivalent to its cores circularly shifting, as follows:

$$(3.6) \quad \dot{\mathcal{T}}^{P_n} = f((\dot{\mathcal{Z}}_n \cdot_L \dots \cdot_L \dot{\mathcal{Z}}_N) \cdot_R (\dot{\mathcal{Z}}_1 \cdot_L \dots \cdot_L \dot{\mathcal{Z}}_{n-1})),$$

with elements

$$(3.7) \quad \begin{aligned} \dot{\mathcal{T}}^{P_n}(i_n, \dots, i_N, i_1, \dots, i_{n-1}) \\ = \text{Tr}\{(\dot{\mathcal{Z}}_n(i_n) \cdot_L \dots \cdot_L \dot{\mathcal{Z}}_N(i_N)) \cdot_R (\dot{\mathcal{Z}}_1(i_1) \cdot_L \dots \cdot_L \dot{\mathcal{Z}}_{n-1}(i_{n-1}))\}. \end{aligned}$$

*Proof.*

$$\begin{aligned}
& \dot{\mathcal{T}}^{P_n}(i_n, \dots, i_N, i_1, \dots, i_{n-1}) \\
&= \sum_{\alpha_1=1}^{r_1} \dots \sum_{\alpha_N=1}^{r_N} \dot{\mathcal{Z}}_1(\alpha_1, i_1, \alpha_2) \cdot_L Z_2(\alpha_2, i_2, \alpha_3) \cdot_L \dots \cdot_L Z_N(\alpha_N, i_N, \alpha_{N+1}) \\
&= \sum_{\alpha_1=1}^{r_1} \dots \sum_{\alpha_N=1}^{r_N} (\dot{\mathcal{Z}}_1(\alpha_1, i_1, \alpha_2) \cdot_L \dots \cdot_L Z_{n-1}(\alpha_{n-1}, i_{n-1}, \alpha_n)) \cdot_L \\
&\quad (Z_n(\alpha_n, i_n, \alpha_{n+1}) \cdot_L \dots \cdot_L Z_N(\alpha_N, i_N, \alpha_{N+1})) \\
&= \sum_{\alpha_1=1}^{r_1} \dots \sum_{\alpha_N=1}^{r_N} (Z_n(\alpha_n, i_n, \alpha_{n+1}) \cdot_L \dots \cdot_L Z_N(\alpha_N, i_N, \alpha_{N+1})) \cdot_R \\
&\quad (\dot{\mathcal{Z}}_1(\alpha_1, i_1, \alpha_2) \cdot_L \dots \cdot_L Z_{n-1}(\alpha_{n-1}, i_{n-1}, \alpha_n)) \\
&= \text{Tr}\{(\dot{\mathcal{Z}}_n(i_n) \cdot_L \dots \cdot_L \dot{\mathcal{Z}}_N(i_N)) \cdot_R (\dot{\mathcal{Z}}_1(i_1) \cdot_L \dots \cdot_L \dot{\mathcal{Z}}_{n-1}(i_{n-1}))\},
\end{aligned} \tag{3.8}$$

where the first equality holds due to (3.5) and (3.2), the second and third equalities hold directly as a result of the definitions of left and right products between quaternion scalars.  $\square$

Although, due to the non-commutativity of quaternion multiplication, there are significant differences in the cyclic permutation property between our defined QTR decomposition and the TR decomposition in [30], they exhibit a similar form, which is why we refer to the decomposition of (3.1) as “quaternion tensor ring”.

**3.1. QTR-QSVD algorithm.** Considering that exact quaternion tensor decompositions often demand extensive computational resources and storage, our focus shifts towards low-rank quaternion tensor approximation within the QTR framework. Inspired by the TR-SVD algorithm for TR decomposition in [30], we propose QTR-QSVD algorithm for learning the QTR model in this section. Before deriving the QTR-QSVD algorithm, we first present a required definition and a required theorem.

**DEFINITION 3.5.** *Quaternion subchain tensors: Several quaternion subchain tensors are defined and denoted by*

$$\begin{aligned}
\dot{\mathcal{Z}}^{<k} &\in \mathbb{H}^{r_1 \times \prod_{n=1}^{k-1} I_n \times r_k} = \dot{\mathcal{Z}}_1 \cdot_L \dot{\mathcal{Z}}_2 \cdot_L \dots \cdot_L \dot{\mathcal{Z}}_{k-1}, \\
\dot{\mathcal{Z}}^{\leq k} &\in \mathbb{H}^{r_1 \times \prod_{n=1}^k I_n \times r_{k+1}} = \dot{\mathcal{Z}}_1 \cdot_L \dot{\mathcal{Z}}_2 \cdot_L \dots \cdot_L \dot{\mathcal{Z}}_k, \\
\dot{\mathcal{Z}}^{>k} &\in \mathbb{H}^{r_{k+1} \times \prod_{n=k+1}^N I_n \times r_1} = \dot{\mathcal{Z}}_{k+1} \cdot_L \dot{\mathcal{Z}}_{k+2} \cdot_L \dots \cdot_L \dot{\mathcal{Z}}_N, \\
\dot{\mathcal{Z}}^{\geq k} &\in \mathbb{H}^{r_k \times \prod_{n=k}^N I_n \times r_1} = \dot{\mathcal{Z}}_k \cdot_L \dot{\mathcal{Z}}_{k+1} \cdot_L \dots \cdot_L \dot{\mathcal{Z}}_N.
\end{aligned} \tag{3.9}$$

Note that the lateral slice matrices of  $\dot{\mathcal{Z}}^{<k}$  are  $\dot{\mathcal{Z}}^{<k}(:, t, :) = \prod_{n=1}^{k-1} \dot{\mathcal{Z}}_n(i_n)$ , where  $t = \overline{i_1 i_2 \dots i_{k-1}}$ . Similar results can be obtained for  $\dot{\mathcal{Z}}^{\leq k}$ ,  $\dot{\mathcal{Z}}^{>k}$ , and  $\dot{\mathcal{Z}}^{\geq k}$ .

**THEOREM 3.6.** *Assume  $\dot{\mathcal{T}}$  can be represented by a QTR decomposition. Then, there is a property that*

$$\dot{\mathbf{T}}_{(k)} = \dot{\mathbf{Z}}_{(2)}^{\leq k} \cdot_L (\dot{\mathbf{Z}}_{[2]}^{>k})^T.$$

*Proof.* Based on the definition of k-unfolding of quaternion tensor  $\dot{\mathcal{T}}$ , we can

express the QTR decomposition in the following form:

$$\begin{aligned}
\dot{\mathbf{T}}_{\langle k \rangle}(t_1, t_2) &= \text{Tr}\{\dot{\mathcal{Z}}_1(i_1) \cdot_L \dot{\mathcal{Z}}_2(i_2) \cdot_L \dots \cdot_L \dot{\mathcal{Z}}_N(i_N)\} \\
&= \text{Tr}\left\{\prod_{n=1}^k \dot{\mathcal{Z}}_n(i_n) \prod_{n=k+1}^N \dot{\mathcal{Z}}_n(i_n)\right\} \\
&= \text{Tr}\left\{\dot{\mathcal{Z}}^{\leq k}(:, t_1, :) \dot{\mathcal{Z}}^{>k}(:, t_2, :)\right\} \\
&= \text{reshape}(\dot{\mathcal{Z}}^{\leq k}(:, t_1, :), [1, r_1 r_{k+1}]) \cdot_L \\
&\quad \text{reshape}((\dot{\mathcal{Z}}^{>k}(:, t_2, :))^T, [r_1 r_{k+1}, 1]) \\
&= \sum_{p=1}^{r_1 r_{k+1}} \dot{\mathbf{Z}}_{(2)}^{\leq k}(t_1, p) \cdot_L ((\dot{\mathbf{Z}}_{[2]}^{>k})^T)(p, t_2),
\end{aligned} \tag{3.10}$$

where  $t_1 = \overline{i_1 i_2 \dots i_k}$  and  $t_2 = \overline{i_{k+1} i_{k+2} \dots i_N}$ . Thus, we have  $\dot{\mathbf{T}}_{\langle k \rangle} = \dot{\mathbf{Z}}_{(2)}^{\leq k} \cdot_L (\dot{\mathbf{Z}}_{[2]}^{>k})^T$ .  $\square$

Now, we present an algorithm that utilizes  $N$  sequential quaternion singular value decompositions (QSVDs) [27] for computing the QTR decomposition. From theorem 3.6, we have  $\dot{\mathbf{T}}_{\langle 1 \rangle} = \dot{\mathbf{Z}}_{(2)}^{\leq 1} \cdot_L (\dot{\mathbf{Z}}_{[2]}^{>1})^T$ , then we truncate the QSVD of  $\dot{\mathbf{T}}_{\langle 1 \rangle}$  to obtain its low-rank approximation, *i.e.*, such that

$$\dot{\mathbf{T}}_{\langle 1 \rangle} = \dot{\mathbf{U}}_1 \Sigma_1 \dot{\mathbf{V}}_1^H + \dot{\varepsilon}_1. \tag{3.11}$$

Let  $\dot{\mathbf{Z}}_{(2)}^{\leq 1} = \dot{\mathbf{U}}_1$  and  $(\dot{\mathbf{Z}}_{[2]}^{>1})^T = \Sigma_1 \dot{\mathbf{V}}_1^H$ , then the first core  $\dot{\mathcal{Z}}_1$  and quaternion subchain tensor  $\dot{\mathcal{Z}}^{>1}$  can be obtained by the proper reshaping and permutation of  $\dot{\mathbf{U}}_1$  and  $\Sigma_1 \dot{\mathbf{V}}_1^H$ , respectively. Afterwards, let  $\dot{\mathbf{Z}}^{>1} = \text{reshape}(\dot{\mathcal{Z}}^{>1}, [r_2 I_2, \prod_{n=3}^N I_n r_1])$ , then truncate the QSVD of  $\dot{\mathbf{Z}}^{>1}$  to obtain its low-rank approximation, *i.e.*, such that

$$\dot{\mathbf{Z}}^{>1} = \dot{\mathbf{U}}_2 \Sigma_2 \dot{\mathbf{V}}_2^H + \dot{\varepsilon}_2. \tag{3.12}$$

Then, the second core  $\dot{\mathcal{Z}}_2$  and quaternion subchain tensor  $\dot{\mathcal{Z}}^{>2}$  can be obtained by the proper reshaping of  $\dot{\mathbf{U}}_2$  and  $\Sigma_2 \dot{\mathbf{V}}_2^H$ , respectively. This procedure can be carried out in a sequential manner to acquire all  $N$  cores  $\dot{\mathcal{Z}}_n, n = 1, 2, \dots, N$ . Similar to the TR-SVD algorithm [30], for QTR-QSVD algorithm, we set the truncation threshold as

$$\delta_n = \begin{cases} \sqrt{2} \epsilon_p \|\dot{\mathcal{T}}\|_F / \sqrt{N}, & n = 1, \\ \epsilon_p \|\dot{\mathcal{T}}\|_F / \sqrt{N}, & n > 1. \end{cases} \tag{3.13}$$

The detailed procedure of the QTR-QSVD algorithm is listed in Algorithm 3.1.

The QTR-QSVD algorithm possesses inherent computational efficiency as a result of its non-recursive nature, enabling it to achieve a high degree of approximation for any given quaternion tensor. We compared the reconstruction (approximation) performance of QTR-QSVD and TR-SVD on color images in Figure 1. Based on the comparison results, we can conclude that the incorporation of quaternions enables QTR-QSVD to achieve better performance in the reconstruction of color images compared to TR-SVD. Similar results can be obtained for other color images as well.

**4. Low-rank quaternion tensor completion.** In this section, we will propose a low-rank quaternion tensor completion model and its corresponding algorithm based on the previously defined QTR decomposition.

**Algorithm 3.1** QTR-QSVD

---

**Input:** An  $N$ -th order quaternion tensor  $\dot{\mathcal{T}} \in \mathbb{H}^{I_1 \times I_2 \times \dots \times I_N}$  and the prescribed relative error  $\epsilon_p$ .

Step1: Compute truncation threshold  $\delta_n$  for  $n = 1$  and  $n > 1$  via (3.13).

Step2: Choose the first mode as the start point and obtain 1-unfolding quaternion matrix  $\dot{\mathbf{T}}_{(1)}$ .

Step3: Low-rank approximation by applying  $\delta_1$ -truncated QSVD:  $\dot{\mathbf{T}}_{(1)} = \dot{\mathbf{U}}_1 \dot{\Sigma}_1 \dot{\mathbf{V}}_1^H + \dot{\varepsilon}_1$ .

Step4: Split ranks  $r_1$  and  $r_2$  by:  $\min_{r_1, r_2} |r_1 - r_2|$ , s.t.  $r_1 r_2 = \text{rank}_{\delta_1}(\dot{\mathbf{T}}_{(1)})$ .

Step5: Obtain  $\dot{\mathcal{Z}}_1$  via  $\dot{\mathcal{Z}}_1 = \text{permute}(\text{reshape}(\dot{\mathbf{U}}_1, [I_1, r_1, r_2]), [2, 1, 3])$ .

Step6: Obtain  $\dot{\mathcal{Z}}^{>1}$  via  $\dot{\mathcal{Z}}^{>1} = \text{permute}(\text{reshape}(\Sigma_1 \dot{\mathbf{V}}_1^H, [r_1, r_2, \prod_{n=2}^N I_n]), [2, 3, 1])$ .

Step7: Perform the following iterative procedure:

for  $n = 2$  to  $N - 1$  do

$\dot{\mathbf{Z}}^{>n-1} = \text{reshape}(\dot{\mathcal{Z}}^{>n-1}, [r_n I_n, \prod_{p=n+1}^N I_p r_1])$ .

Compute  $\delta_n$ -truncated QSVD:  $\dot{\mathbf{Z}}^{>n-1} = \dot{\mathbf{U}}_n \dot{\Sigma}_n \dot{\mathbf{V}}_n^H + \dot{\varepsilon}_n$ .

$r_{n+1} = \text{rank}_{\delta_n}(\dot{\mathbf{Z}}^{>n-1})$ .

$\dot{\mathcal{Z}}_n = \text{reshape}(\dot{\mathbf{U}}_n, [r_n, I_n, r_{n+1}])$ .

$\dot{\mathcal{Z}}^{>n} = \text{reshape}(\Sigma_n \dot{\mathbf{V}}_n^H, [r_{n+1}, \prod_{p=n+1}^N I_p, r_1])$ .

end for

**Output:**  $N$  cores  $\dot{\mathcal{Z}}_n, n = 1, 2, \dots, N$  of QTR decomposition.

---

**4.1. LRQTC model based on QTR weighted nuclear norm minimization.**

In order to introduce the QTR weighted nuclear norm formulation, we first define the circular unfolding of a quaternion tensor and then theoretically establish its connection to the QTR-rank.

**DEFINITION 4.1.** *Quaternion tensor circular unfolding: Let  $\dot{\mathcal{T}} \in \mathbb{H}^{I_1 \times I_2 \times \dots \times I_N}$  be an  $N$ -th order quaternion tensor, its circular unfolding is a quaternion matrix, denoted by  $\dot{\mathbf{T}}_{\{k,l\}}$ , which first permutes  $\dot{\mathcal{T}}$  with order  $[k, \dots, N, 1, \dots, k-1]$  and then performs matricization along the first  $l$  modes, i.e.,  $l$ -unfolding. The indices of  $\dot{\mathbf{T}}_{\{k,l\}}(p, q)$  are formulated as*

$$(4.1) \quad \dot{\mathbf{T}}_{\{k,l\}}(p, q) = \dot{\mathcal{T}}(i_1, i_2, \dots, i_N),$$

where  $p = 1 + \sum_{s=k}^{k+l-1} (i_s - 1) \prod_{t=k}^{s-1} I_t$  and  $q = 1 + \sum_{s=k+l}^{k-1} (i_s - 1) \prod_{t=k+l}^{s-1} I_t$ .

Note that when  $l = 1$ , the quaternion tensor circular unfolding is reduced to the quaternion tensor mode- $k$  unfolding of  $\dot{\mathcal{T}}$ , i.e.,  $\dot{\mathbf{T}}_{\{k,1\}} = \dot{\mathbf{T}}_{[k]}$ .

**THEOREM 4.2.** *Assume that  $\dot{\mathcal{T}} \in \mathbb{H}^{I_1 \times I_2 \times \dots \times I_N}$  is an  $N$ -th order quaternion tensor with QTR-rank  $\mathbf{r} = [r_1, r_2, \dots, r_N]$ , and then when  $l = N - k + 1$ , for each  $\dot{\mathbf{T}}_{\{k,l\}}$ , we have*

$$(4.2) \quad \text{rank}(\dot{\mathbf{T}}_{\{k,l\}}) \leq r_k r_{k+l}.$$

*Proof.* From (3.1) and (4.1),  $\dot{\mathbf{T}}_{\{k,l\}}(p, q)$  can be represented in the index form, that is

$$(4.3) \quad \dot{\mathbf{T}}_{\{k,l\}}(p, q) = \dot{\mathcal{T}}(i_1, i_2, \dots, i_N) = \text{Tr}\{\dot{\mathcal{Z}}_1(i_1) \cdot_L \dot{\mathcal{Z}}_2(i_2) \cdot_L \dots \cdot_L \dot{\mathcal{Z}}_N(i_N)\}.$$

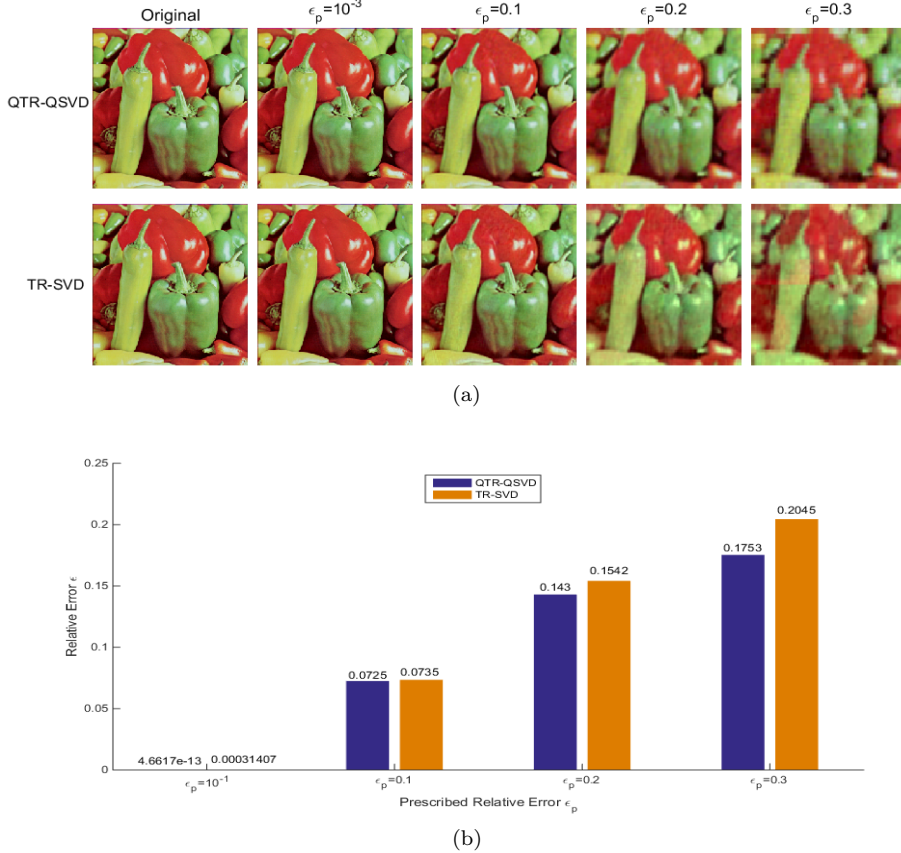


FIG. 1. The reconstruction of one color image “peppers” by using QTR-QSVD and TR-SVD. The color image is tensorized to 9th-order quaternion tensor  $4 \times 4 \times \dots \times 4$  (10th-order tensor  $4 \times 4 \times \dots \times 4 \times 3$  for TR-SVD) by the OKA procedure (see Section 5). (a) The reconstruction results are visually displayed for different prescribed relative errors. (b) The reconstruction relative errors are shown for different prescribed relative errors.

When  $l = N - k + 1$ , (4.3) can be rewritten as

$$\begin{aligned}
 (4.4) \quad & \dot{\mathbf{T}}_{\{k,l\}}(p, q) = \text{Tr}\{\dot{\mathcal{Z}}_k(i_k) \cdot_L \dots \cdot_L \dot{\mathcal{Z}}_N(i_N) \cdot_R (\dot{\mathcal{Z}}_1(i_1) \cdot_L \dots \cdot_L \dot{\mathcal{Z}}_{k-1}(i_{k-1}))\} \\
 & = \text{Tr}\{\dot{\mathcal{Z}}_k(i_k) \cdot_L \dots \cdot_L \dot{\mathcal{Z}}_{k+l-1}(i_{k+l-1}) \cdot_R (\dot{\mathcal{Z}}_1(i_1) \cdot_L \dots \cdot_L \dot{\mathcal{Z}}_{k-1}(i_{k-1}))\} \\
 & = \text{Tr}\{\dot{\mathcal{W}}(:, p, :) \cdot_R \dot{\mathcal{H}}(:, q, :)\} \\
 & = \sum_{\alpha_1=1}^{r_k} \sum_{\alpha_2=1}^{r_{l+k}} \dot{\mathcal{W}}(\alpha_1, p, \alpha_2) \cdot_R \dot{\mathcal{H}}(\alpha_2, q, \alpha_1) \\
 & = \sum_{\beta=1}^{r_k r_{l+k}} \dot{\mathbf{W}}_{(2)}(p, \beta) \cdot_R \dot{\mathbf{H}}_{[2]}^T(\beta, q) \\
 & = \sum_{\beta=1}^{r_k r_{l+k}} \dot{\mathbf{H}}_{[2]}^T(\beta, q) \dot{\mathbf{W}}_{(2)}(p, \beta),
 \end{aligned}$$

where  $\dot{\mathcal{W}} \in \mathbb{H}^{r_k \times \prod_{n=k}^N I_n \times r_{l+k}} = \dot{\mathcal{Z}}_k \cdot_L \dots \cdot_L \dot{\mathcal{Z}}_{k+l-1}$ ,  $\dot{\mathcal{H}} \in \mathbb{H}^{r_1 \times \prod_{n=1}^{k-1} I_n \times r_k} = \dot{\mathcal{Z}}_1 \cdot_L \dots \cdot_L \dot{\mathcal{Z}}_{k-1}$ . According to (4.4), we can get that  $\dot{\mathbf{T}}_{\{k,l\}} = \dot{\mathbf{W}}_{(2) \cdot R} \dot{\mathbf{H}}_{[2]}^T$ , which combining (2.4) means  $\text{rank}(\dot{\mathbf{T}}_{\{k,l\}}) \leq \min(\text{rank}(\dot{\mathbf{W}}_{(2)}), \text{rank}(\dot{\mathbf{H}}_{[2]}^T)) \leq \min(r_k r_{k+l}, \prod_{n=k}^N I_n, \prod_{n=1}^{k-1} I_n)$ . Note that  $r_{k+l} = r_{N+1} = r_1$ .  $\square$

**4.1.1. The proposed model.** From Theorem 4.2, we can observe that for an arbitrary  $N$ -th order quaternion tensor with QTR-rank  $\mathbf{r} = [r_1, r_2, \dots, r_N]$ , the rank of each circular unfolding quaternion matrix  $\dot{\mathbf{T}}_{\{k,l\}}$  with  $l = N - k + 1$  is bounded by  $r_k r_{k+l}$ . Hence, the problem of quaternion tensor QTR-rank minimization can be equivalently transformed into a sequence of quaternion matrix rank minimization subproblems, *i.e.*, to minimize QTR-rank, a natural option is to consider the sum of rank of circular unfolding quaternion matrices:

$$(4.5) \quad \min_{\dot{\mathcal{T}}} \sum_{k=2}^N \alpha_k \text{rank}(\dot{\mathbf{T}}_{\{k,l\}}),$$

where  $\alpha_k$  for  $k = 2, 3, \dots, N$  are positive parameters satisfying  $\sum_{k=2}^N \alpha_k = 1$ . Note that  $k$  starts from 2, because when  $k = 1$ , there is no permutation for  $\dot{\mathcal{T}}$ . Nevertheless, the general computational complexity of problem (4.5) makes it intractable. To address the solvability of (4.5), a convex surrogate, the sum of weighted nuclear norm, has been adopted. The definition of this surrogate is provided as follows.

**DEFINITION 4.3.** *QTR weighted nuclear norm: Assume the quaternion tensor  $\dot{\mathcal{T}}$  with QTR decomposition, its QTR weighted nuclear norm is defined as*

$$(4.6) \quad \text{Qtrwnn} = \sum_{k=2}^N \alpha_k \|\dot{\mathbf{T}}_{\{k,l\}}\|_{w,*},$$

where  $l = N - k + 1$ .

Based on the definition of QTR weighted nuclear norm (4.6), we propose the following LRQTC model:

$$(4.7) \quad \begin{aligned} & \min_{\dot{\mathcal{T}}} \sum_{k=2}^N \alpha_k \|\dot{\mathbf{T}}_{\{k,l\}}\|_{w,*} \\ & \text{s.t. } P_{\Omega}(\dot{\mathcal{T}}) = P_{\Omega}(\dot{\mathcal{X}}), \end{aligned}$$

where  $\dot{\mathcal{T}} \in \mathbb{H}^{I_1 \times I_2 \times \dots \times I_N}$  is a completed output  $N$ -th order quaternion tensor,  $\dot{\mathcal{X}} \in \mathbb{H}^{I_1 \times I_2 \times \dots \times I_N}$  is the observed  $N$ -th order quaternion tensor, and  $P_{\Omega}(\cdot)$  is the projection operator on  $\Omega$  which is the index of observed elements. Specifically,

$$\mathcal{P}_{\Omega}(\dot{\mathcal{T}}) = \begin{cases} \dot{\mathcal{T}}(i_1, i_2, \dots, i_N), & (i_1, i_2, \dots, i_N) \in \Omega, \\ 0, & \text{otherwise.} \end{cases}$$

**4.1.2. Solving algorithm.** To enable the solution of (4.7), we use the variable-splitting technique and introduce auxiliary quaternion tensors  $\{\dot{\mathcal{M}}^{(k)}\}_{k=2}^N \in \mathbb{H}^{I_1 \times I_2 \times \dots \times I_N}$  in (4.7). Consequently, (4.7) is finally transformed into the following solvable model:

$$(4.8) \quad \begin{aligned} & \min_{\dot{\mathcal{T}}, \{\dot{\mathcal{M}}^{(k)}\}} \sum_{k=2}^N \alpha_k \|\dot{\mathbf{M}}_{\{k,l\}}^{(k)}\|_{w,*} \\ & \text{s.t. } \dot{\mathcal{T}} = \dot{\mathcal{M}}^{(k)}, \quad k = 2, 3, \dots, N, \\ & \quad P_{\Omega}(\dot{\mathcal{T}}) = P_{\Omega}(\dot{\mathcal{X}}). \end{aligned}$$

Based on the ADMM framework in the quaternion domain [12], the augmented Lagrangian function of (4.8) is defined as

$$(4.9) \quad \begin{aligned} \mathcal{L}_\mu(\dot{\mathcal{X}}, \{\dot{\mathcal{M}}^{(k)}\}_{k=2}^N, \{\dot{\mathcal{Y}}^{(k)}\}_{k=2}^N) &= \sum_{k=2}^N \alpha_k \|\dot{\mathbf{M}}_{\{k,l\}}^{(k)}\|_{w,*} + \Re(\langle \dot{\mathcal{Y}}^{(k)}, \dot{\mathcal{T}} - \dot{\mathcal{M}}^{(k)} \rangle) \\ &\quad + \frac{\mu_k}{2} \|\dot{\mathcal{T}} - \dot{\mathcal{M}}^{(k)}\|_F^2 \\ \text{s.t. } P_\Omega(\dot{\mathcal{T}}) &= P_\Omega(\dot{\mathcal{X}}), \end{aligned}$$

where  $\dot{\mathcal{Y}}^{(k)} \in \mathbb{H}^{I_1 \times I_2 \times \dots \times I_N}$  for  $k = 2, 3, \dots, N$  are Lagrange Multipliers,  $\mu_k > 0$  for  $k = 2, 3, \dots, N$  are penalty parameters. Then, we use an iterative scheme to solve the problem (4.9).

**Update  $\dot{\mathcal{M}}^{(k)}$ :** To optimize  $\dot{\mathcal{M}}^{(k)}$  is equivalent to solve the subproblem:

$$(4.10) \quad \begin{aligned} \dot{\mathcal{M}}^{(k)} &= \arg \min_{\dot{\mathcal{M}}^{(k)}} \alpha_k \|\dot{\mathbf{M}}_{\{k,l\}}^{(k)}\|_{w,*} + \Re(\langle \dot{\mathcal{Y}}^{(k)}, \dot{\mathcal{T}} - \dot{\mathcal{M}}^{(k)} \rangle) + \frac{\mu_k}{2} \|\dot{\mathcal{T}} - \dot{\mathcal{M}}^{(k)}\|_F^2 \\ &= \arg \min_{\dot{\mathcal{M}}^{(k)}} \frac{\alpha_k}{\mu_k} \|\dot{\mathbf{M}}_{\{k,l\}}^{(k)}\|_{w,*} + \frac{1}{2} \|\dot{\mathcal{M}}^{(k)} - (\dot{\mathcal{T}} + \frac{\dot{\mathcal{Y}}^{(k)}}{\mu_k})\|_F^2. \end{aligned}$$

Denote  $\dot{\Gamma} = \dot{\mathcal{T}} + \frac{\dot{\mathcal{Y}}^{(k)}}{\mu_k}$  and let  $\dot{\Gamma} = \dot{\mathbf{U}} \dot{\Sigma} \dot{\mathbf{V}}^H$  be the QSVD of  $\dot{\Gamma}$ , where

$$\dot{\Sigma} = \begin{bmatrix} \text{diag}(\sigma_1(\dot{\Gamma}), \dots, \sigma_s(\dot{\Gamma})) \\ \mathbf{0} \end{bmatrix},$$

and  $\sigma_n(\dot{\Gamma})$  is the  $n$ -th singular value of  $\dot{\Gamma}$ ,  $s$  denotes the number of nonzero singular values of  $\dot{\Gamma}$ . From [25], the problem (4.10) has the following closed-form solution:

$$(4.11) \quad \dot{\mathcal{M}}^{(k)} = \text{fold}_{\{k,l\}}(\dot{\mathbf{U}} \dot{\Sigma} \dot{\mathbf{V}}^H),$$

where

$$\hat{\Sigma} = \begin{bmatrix} \text{diag}(\sigma_1(\dot{\mathbf{M}}_{\{k,l\}}^{(k)}), \dots, \sigma_s(\dot{\mathbf{M}}_{\{k,l\}}^{(k)})) \\ \mathbf{0} \end{bmatrix},$$

and  $\sigma_n(\dot{\mathbf{M}}_{\{k,l\}}^{(k)}) = \begin{cases} 0, & \text{if } c_2 < 0 \\ \frac{c_1 + \sqrt{c_2}}{2}, & \text{if } c_2 \geq 0 \end{cases}$ , with  $c_1 = \sigma_n(\dot{\Gamma}) - \epsilon$ ,  $c_2 = (\sigma_n(\dot{\Gamma}) + \epsilon)^2 - 4C$ , and  $C$  is a compromising constant.

**Update  $\dot{\mathcal{T}}$ :** To optimize  $\dot{\mathcal{T}}$  is equivalent to solve the subproblem:

$$(4.12) \quad \begin{aligned} \dot{\mathcal{T}} &= \arg \min_{P_\Omega(\dot{\mathcal{T}}) = P_\Omega(\dot{\mathcal{X}})} \sum_{k=2}^N \Re(\langle \dot{\mathcal{Y}}_k, \dot{\mathcal{T}} - \dot{\mathcal{M}}^{(k)} \rangle) + \frac{\mu_k}{2} \|\dot{\mathcal{T}} - \dot{\mathcal{M}}^{(k)}\|_F^2 \\ &= \arg \min_{P_\Omega(\dot{\mathcal{X}}) = P_\Omega(\dot{\mathcal{T}})} \sum_{k=2}^N \frac{\mu_k}{2} \|\dot{\mathcal{T}} - \dot{\mathcal{M}}^{(k)} + \frac{\dot{\mathcal{Y}}^{(k)}}{\mu_k}\|_F^2 \end{aligned}$$

It is easy to check that the solution of (4.12) is given by:

$$(4.13) \quad \dot{\mathcal{T}} = P_{\Omega^c} \left( \frac{\sum_{k=2}^N (\dot{\mathcal{M}}^{(k)} - \frac{\dot{\mathcal{Y}}^{(k)}}{\mu_k})}{N-1} \right) + P_\Omega(\dot{\mathcal{X}}),$$

where  $\Omega^c$  is the complement of  $\Omega$ .

**Update  $\dot{\mathcal{Y}}^{(k)}$ :** The Lagrange multiplier  $\dot{\mathcal{Y}}^{(k)}$  is updated by:

$$(4.14) \quad \dot{\mathcal{Y}}^{(k)} = \dot{\mathcal{Y}}^{(k)} + \mu_k(\dot{\mathcal{T}} - \dot{\mathcal{M}}^{(k)}).$$

To speed up convergence, each iteration we also update  $\mu_k$  by:  $\mu_k = \min(\mu_{max}, \rho\mu_k)$ , where  $\mu_{max}$  is the default maximum of  $\mu_k$ ,  $\rho > 1$  is a constant parameter.

Finally, the proposed LRQTC algorithm is summarized in Algorithm 4.1.

---

**Algorithm 4.1** Our proposed LRQTC algorithm.

---

**Input:** The observed  $N$ -th order quaternion tensor  $\dot{\mathcal{T}} \in \mathbb{H}^{I_1 \times I_2 \times \dots \times I_N}$  with  $\Omega$  (the index of observed elements),  $\{\alpha_k\}_{k=2}^N$ ,  $\mu_{max}$  and  $\rho$ .  
**Initialize**  $\{\dot{\mathcal{M}}^{(k)}\}_{k=2}^N$ ,  $\{\dot{\mathcal{Y}}^{(k)}\}_{k=2}^N$ , and  $\{\mu_k\}_{k=2}^N$ .  
**Repeat**  
**for**  $k = 2$  to  $N$  **do**  
    Update  $\dot{\mathcal{M}}^{(k)}$  via (4.11);  
**end for**  
    Update  $\dot{\mathcal{T}}$  via (4.13) (the updated one is labeled by  $\tilde{\mathcal{T}}$ ).  
**for**  $k = 2$  to  $N$  **do**  
    Update  $\dot{\mathcal{Y}}^{(k)}$  via (4.14);  
    Update  $\mu_k$  via  $\mu_k = \min(\mu_{max}, \rho\mu_k)$ .  
**end for**  
**Until**  $\frac{\|\dot{\mathcal{T}} - \tilde{\mathcal{T}}\|_F}{\|\tilde{\mathcal{T}}\|_F} < 10^{-5}$  or reach the preset maximum number of iterations.

**Output:** The recovered quaternion tensor  $\tilde{\mathcal{T}}$ .

---

**5. Color image inpainting.** In this section, we will elaborate on how to utilize the proposed LRQTC model for color image inpainting. Because a color image is essentially a quaternion matrix (a second-order quaternion tensor), it is necessary to increase the order of the quaternion matrix in order to effectively utilize the proposed LRQTC method. Recently, the overlapping ket augmentation (OKA) as a tensor augmentation technique was developed in [28] for increasing the order of tensors. OKA is an improvement upon KA [1] as it overcomes the visual flaws caused by reshaping and eliminates the blocking artifacts introduced by KA. Therefore, in order to increase the order of quaternion matrices used for representing color images, we apply OKA to tensors [28] and quaternion matrices. Due to the similarity in the process of applying OKA to tensors [28] and quaternion matrices, we will not reiterate it here. Finally, we summarize the entire process of color image inpainting in Figure 2.

**6. Experimental results.** To validate the effectiveness of our color image inpainting method, we conducted extensive experiments using a diverse range of images, including natural color images, color medical images, and color face images. We compare our proposed method with several classic and state-of-the-art quaternion matrix and tensor completion methods, including t-SVD [29], TMac-TT [1], TRLRF [26], TRNNM [6], LRQA-2 [3], LRQMC [13], and TQLNA [24]. In order to assess the performance of the proposed method, we considered not only visual quality but also utilized two commonly used quantitative quality metrics: peak signal-to-noise ratio (PSNR) and structural similarity (SSIM) [22]. All the experiments are run in MATLAB 2014b under Windows 10 on a personal computer with a 1.60GHz CPU and 8GB memory.

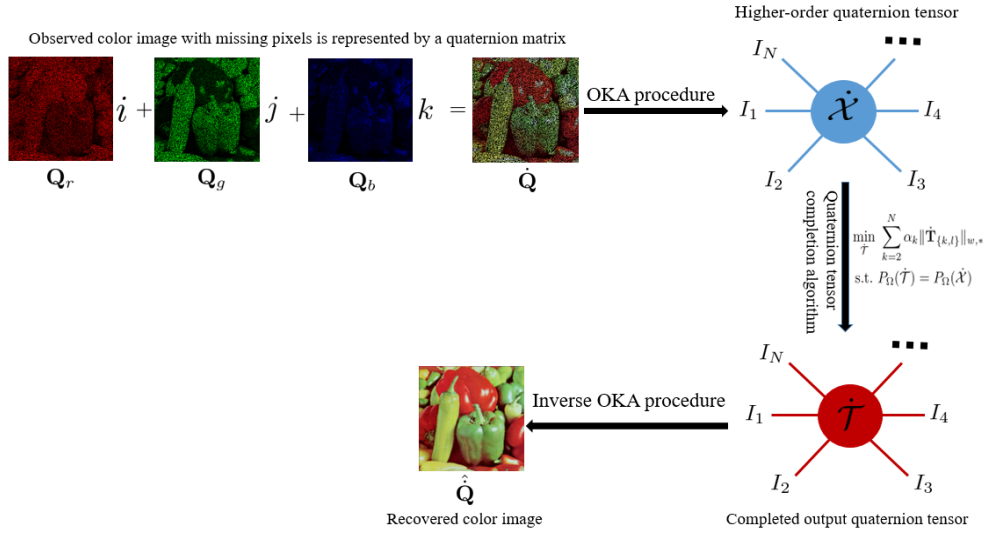


FIG. 2. The entire process of color image inpainting.

**6.1. Natural color image inpainting.** Five natural color images (shown in the first row of figure 3) with a spatial resolution of  $256 \times 256$  are utilized for the evaluation. For our proposed method, the color images are transformed into ninth-order quaternion tensors of size  $4 \times 4 \times 4$  using OKA. We set  $\alpha_k = \frac{\omega_k}{\sum_{k=2}^N \omega_k}$  with  $\omega_k = \min(\prod_{n=1}^{k-1} I_n, \prod_{n=k}^N I_n)$  for  $k = 2, 3, \dots, N$ ,  $\mu_{\max} = 10^6$ , and  $\rho = 1.03$ . We initialize  $\dot{\mathcal{M}}^{(k)} = \dot{\mathcal{T}}, \dot{\mathcal{Y}}^{(k)} = \mathbf{0}$  for  $k = 2, 3, \dots, N$ , and  $\mu = \{0.5, 0.5, 0.001, 10^{-4}, 1, 10^{-4}, 1, 0.001, 0.5, 0.5\}$ . Furthermore, all the compared methods were implemented using their source codes, and the parameter configurations were set according to the recommendations provided in the original papers.

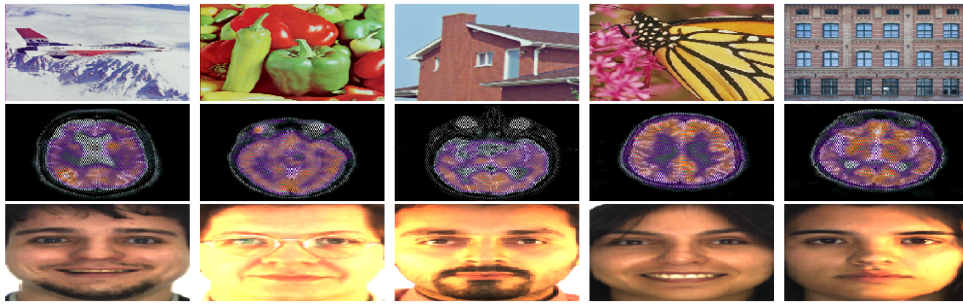


FIG. 3. The tested natural color images, color medical images, and color face images.

## 6.2. Color medical images.

## 6.3. Color face images.

## 7. Conclusions.

**Acknowledgments.** We would like to acknowledge.

## REFERENCES

- [1] J. A. BENGUA, H. N. PHIEN, H. D. TUAN, AND M. N. DO, *Efficient tensor completion for color image and video recovery: Low-rank tensor train*, IEEE Transactions on Image Processing, 26 (2017), pp. 2466–2479.
- [2] Y. CHEN, L. QI, X. ZHANG, AND Y. XU, *A low rank quaternion decomposition algorithm and its application in color image inpainting*, arXiv preprint arXiv:2009.12203, (2020).
- [3] Y. CHEN, X. XIAO, AND Y. ZHOU, *Low-rank quaternion approximation for color image processing*, IEEE Transactions on Image Processing, 29 (2019), pp. 1426–1439.
- [4] A. CICHOCKI, D. MANDIC, L. DE LATHAUWER, G. ZHOU, Q. ZHAO, C. CAIAFA, AND H. A. PHAN, *Tensor decompositions for signal processing applications: From two-way to multi-way component analysis*, IEEE signal processing magazine, 32 (2015), pp. 145–163.
- [5] W. R. HAMILTON, *Elements of quaternions*, Longmans, Green, & Company, 1866.
- [6] H. HUANG, Y. LIU, J. LIU, AND C. ZHU, *Provable tensor ring completion*, Signal Processing, 171 (2020), p. 107486.
- [7] H. HUANG, Y. LIU, Z. LONG, AND C. ZHU, *Robust low-rank tensor ring completion*, IEEE Transactions on Computational Imaging, 6 (2020), pp. 1117–1126.
- [8] Z. JIA, Q. JIN, M. K. NG, AND X.-L. ZHAO, *Non-local robust quaternion matrix completion for large-scale color image and video inpainting*, IEEE Transactions on Image Processing, 31 (2022), pp. 3868–3883.
- [9] Z. JIA, M. K. NG, AND G.-J. SONG, *Robust quaternion matrix completion with applications to image inpainting*, Numerical Linear Algebra with Applications, 26 (2019), p. e2245.
- [10] T. G. KOLDA AND B. W. BADER, *Tensor decompositions and applications*, SIAM review, 51 (2009), pp. 455–500.
- [11] H. LI, Z. LIU, Y. HUANG, AND Y. SHI, *Quaternion generic fourier descriptor for color object recognition*, Pattern recognition, 48 (2015), pp. 3895–3903.
- [12] J. MIAO AND K. I. KOU, *Quaternion-based bilinear factor matrix norm minimization for color image inpainting*, IEEE Trans. Signal Process., 68 (2020), pp. 5617–5631.
- [13] J. MIAO AND K. I. KOU, *Color image recovery using low-rank quaternion matrix completion algorithm*, IEEE Transactions on Image Processing, 31 (2021), pp. 190–201.
- [14] J. MIAO, K. I. KOU, AND W. LIU, *Low-rank quaternion tensor completion for recovering color videos and images*, Pattern Recognition, 107 (2020), p. 107505.
- [15] J. MIAO, K. I. KOU, L. YANG, AND D. CHENG, *Quaternion tensor train rank minimization with sparse regularization in a transformed domain for quaternion tensor completion*, arXiv preprint arXiv:2209.02964, (2022).
- [16] J. MIAO, K. I. KOU, L. YANG, AND J. HAN, *Quaternion matrix completion using untrained quaternion convolutional neural network for color image inpainting*, arXiv preprint arXiv:2305.00416, (2023).
- [17] I. V. OSELEDETS, *Tensor-train decomposition*, SIAM Journal on Scientific Computing, 33 (2011), pp. 2295–2317.
- [18] Z. QIN, Z. MING, AND L. ZHANG, *Singular value decomposition of third order quaternion tensors*, Applied Mathematics Letters, 123 (2022), p. 107597.
- [19] Y. QIU, G. ZHOU, Q. ZHAO, AND S. XIE, *Noisy tensor completion via low-rank tensor ring*, IEEE Transactions on Neural Networks and Learning Systems, (2022).
- [20] D. SCHULZ, J. SEITZ, AND J. P. C. L. DA COSTA, *Widely linear simo filtering for hypercomplex numbers*, in 2011 IEEE Information Theory Workshop, IEEE, 2011, pp. 390–395.
- [21] D. SCHULZ AND R. S. THOMÄ, *Using quaternion-valued linear algebra*, arXiv preprint arXiv:1311.7488, (2013).
- [22] Z. WANG, A. C. BOVIK, H. R. SHEIKH, AND E. P. SIMONCELLI, *Image quality assessment: from error visibility to structural similarity*, IEEE transactions on image processing, 13 (2004), pp. 600–612.
- [23] P.-L. WU, X.-L. ZHAO, M. DING, Y.-B. ZHENG, L.-B. CUI, AND T.-Z. HUANG, *Tensor ring decomposition-based model with interpretable gradient factors regularization for tensor completion*, Knowledge-Based Systems, 259 (2023), p. 110094.
- [24] L. YANG, J. MIAO, AND K. I. KOU, *Quaternion-based color image completion via logarithmic approximation*, Information Sciences, 588 (2022), pp. 82–105.
- [25] Y. YU, Y. ZHANG, AND S. YUAN, *Quaternion-based weighted nuclear norm minimization for color image denoising*, Neurocomputing, 332 (2019), pp. 283–297.
- [26] L. YUAN, C. LI, D. MANDIC, J. CAO, AND Q. ZHAO, *Tensor ring decomposition with rank*

*minimization on latent space: An efficient approach for tensor completion*, in Proceedings of the AAAI conference on artificial intelligence, vol. 33, 2019, pp. 9151–9158.

[27] F. ZHANG, *Quaternions and matrices of quaternions*, Linear algebra and its applications, 251 (1997), pp. 21–57.

[28] Y. ZHANG, Y. WANG, Z. HAN, Y. TANG, ET AL., *Effective tensor completion via element-wise weighted low-rank tensor train with overlapping ket augmentation*, IEEE Transactions on Circuits and Systems for Video Technology, 32 (2022), pp. 7286–7300.

[29] Z. ZHANG AND S. AERON, *Exact tensor completion using t-svd*, IEEE Transactions on Signal Processing, 65 (2016), pp. 1511–1526.

[30] Q. ZHAO, G. ZHOU, S. XIE, L. ZHANG, AND A. CICHOCKI, *Tensor ring decomposition*, arXiv preprint arXiv:1606.05535, (2016).

[31] Y.-B. ZHENG, T.-Z. HUANG, X.-L. ZHAO, Q. ZHAO, AND T.-X. JIANG, *Fully-connected tensor network decomposition and its application to higher-order tensor completion*, in Proceedings of the AAAI conference on artificial intelligence, vol. 35, 2021, pp. 11071–11078.